

# Theoretical Study of Electronic Structure and Superconductivity in $Nb_{1-x}B_2$ Alloys

P. Jiji Thomas Joseph and Prabhakar P. Singh

*Department of Physics, Indian Institute of Technology, Powai, Mumbai-400076, India*

---

## Abstract

Using the Korringa-Kohn-Rostoker coherent-potential approximation in the atomic-sphere approximation (KKR-ASA CPA) we have studied the changes in the electronic structure and the superconducting transition temperature  $T_c$  in  $Nb_{1-x}B_2$  alloys as a function of  $x$ . We find that the variation in the electronic structure of  $Nb_{1-x}B_2$  alloys as a function of  $x$  is consistent with the rigid-band model. However, the variation of  $T_c$ , obtained using the Allen-Dynes equation within the Gaspari-Gyorffy formalism to estimate the electron-phonon matrix elements, does not follow the expected trend. We associate this disagreement to the use of a constant  $\omega_{rms}$  in the Allen-Dynes equation over the whole range of vacancy concentration, thereby indicating the importance of lattice dynamical effects in these systems.

*Key words:*

electronic structure, alloys, superconductivity

PACS: 74.25.Kc, 63.20.Kr

---

## 1 INTRODUCTION

The discovery of superconductivity in  $MgB_2$  and the fact that the carbides and the nitrides of  $Nb$  show superconductivity have renewed interest in finding superconductivity in the borides of  $Nb$ , in particular, the diborides. However, the search for superconductivity in  $NbB_2$  and  $NbB_2$ -based alloys is not new. Earlier work by Zeigler *et al* [1] and Hulm *et al* [2] showed  $B$  deficient  $NbB_2$ , namely  $NbB_{1.94}$  to be superconducting with superconducting transition temperature,  $T_c$ , of around 1.2 K, while Schriber *et al* [3] found  $NbB_x$  (synthesized under pressure) with  $x \sim 2$  to be superconducting with  $T_c$  of 9.2 K.

Recently, Yamamoto *et al* [4] and Kotegawa *et al* [5] have reported superconductivity in  $Nb_{1-x}B_2$  alloys when synthesized under pressure for  $x$  ranging from 0 to 0.48. They find that  $Nb_{1-x}B_2$  samples become superconducting for  $x = 0.04$ , and

the  $T_c$  increases to around 9.2 K for  $x = 0.24$ , thereafter  $T_c$  remains essentially unchanged up to  $x = 0.48$ .

In an effort to theoretically understand the changes in the electronic structure of  $Nb_{1-x}B_2$  and  $NbB_{1.94}$  alloys and their superconducting properties as vacancies are introduced either in the  $Nb$  plane or the  $B$  plane, we have carried out first-principles electronic structure calculations of these alloys as a function of vacancy concentration. We have used Korringa-Kohn-Rostoker coherent-potential approximation [6,7] in the atomic-sphere approximation (KKR-ASA CPA) method for taking into account the effects of disorder, Gaspari-Gyorffy formalism [8] for calculating the electron-phonon coupling constant  $\lambda$ , and Allen-Dynes equation [9] for calculating  $T_c$  in  $Nb_{1-x}B_2$  and  $NbB_{1.94}$  alloys.

Here, we like to point out that the recent theoretical work of Shein *et al* [10] to model disordered  $Nb_{0.75}B_2$  alloy using a 12-atom supercell may not be adequate. This can be seen as follows. Each metal atom in  $AlB_2$ -type diborides has  $D_{6h}$  symmetry and thus has 12  $B$  neighbors at the vertices of a hexagonal prism. In addition, the central metal atom also sees 8 others through the faces of the  $B_{12}$  prism at a distance comparable with the metallic diameter. Thus a minimum of 24-atom supercell would have been more appropriate. However, their conclusion that the superconductivity in  $Nb_{1-x}B_2$  alloys is governed more by the changes that take place in the lattice properties when vacancies are introduced in the metal plane of the diborides, is consistent with our results. Before describing our results, we provide some of the computational details of the present approach.

## 2 Computational Details

### 2.1 The densities of states

The charge self-consistent electronic structure of  $Nb_{1-x}B_2$  and  $NbB_{1.93}$  alloys has been calculated using the KKR-ASA CPA method with  $x$  ranging from 0 to 0.48. The lattice constants for  $Nb_{1-x}B_2$  alloys are taken from the experimental work of Yamamoto *et al*[4]. To determine the electronic structure of  $NbB_2$  using the present approach, we have used the lattice constants  $a$  and  $c$  from our earlier full-potential linear muffin-tin orbital calculations[11]. The absence of  $Nb$  and  $B$  atoms in the  $Nb$  and  $B$  planes, respectively, were modelled by introducing empty spheres at those sites. The disorder was accounted for by the coherent-potential approximation [12,13,14], which has been very successful in describing reliably many physical properties of disordered alloys [7]. The exchange-correlation potential was parametrized as suggested by Perdew-Wang within the generalized gradient approximation [15,16]. The Brillouin zone (BZ) integration was carried out with 1215  $\mathbf{k}$ -points in the irreducible part of the BZ. For densities of states (DOS) calcu-

lations, we added a small imaginary component of 1 *mRy* to the energy and used 4900 **k**-points in the irreducible part of the BZ. For valence states the angular momentum cut-off was kept as  $l_{max} = 3$ , and the core states were recalculated. For *Nb* and *B* the ratio of the atomic sphere radius to the Wigner-Seitz radius was kept fixed at 1.294 and 0.747, respectively. The empty spheres inherited the radii of the corresponding atomic spheres. The present calculations were carried out using the scalar-relativistic Schroedinger equation. The Green's function is calculated in a complex plane with a 20 point Gaussian quadrature.

## 2.2 The electron-phonon coupling and the superconducting transition temperature

The superconducting transition temperature  $T_c$  was calculated with the Allen-Dynes equation,

$$T_c = \frac{\omega_{ln}}{1.2} \exp \left[ -\frac{1.04(1 + \lambda)}{\lambda - \mu^*(1 + 0.62\lambda)} \right]. \quad (1)$$

In our calculation, the value of the phonon frequency  $\omega_{ln}$  for *NbB<sub>2</sub>* was taken from Ref. [11],  $\mu^*$  was set equal to 0.09, and the electron-phonon coupling constant  $\lambda$  was calculated using the Gaspari-Gyorffy formalism with the charge self-consistent potentials of *Nb<sub>1-x</sub>B<sub>2</sub>* and *NbB<sub>1.93</sub>* alloys obtained with the KKR-ASA CPA method. This entails writing  $\lambda$  in terms of Hopfield parameter,  $\eta$ , as

$$\lambda = \sum_i \frac{\eta_i}{M_i \langle \omega_i^2 \rangle}, \quad (2)$$

where the sum is over the basis atoms in the primitive cell,  $M$  is the atomic mass and  $\langle \omega^2 \rangle^{1/2}$  is an average phonon frequency. The average phonon frequency  $\langle \omega^2 \rangle^{1/2}$  is taken to be the root-mean-square frequency  $\omega_{rms} = \langle \omega^2 \rangle^{1/2}$ . In the Gaspari-Gyorffy formalism the spherically averaged Hopfield parameter is given by

$$\eta = 2 \sum_l \frac{(l+1)}{(2l+1)(2l+3)} M_{l,l+1}^2 \frac{N_l(E_F)N_{l+1}(E_F)}{N(E_F)}. \quad (3)$$

The total DOS at the Fermi energy  $E_F$ ,  $N(E_F)$ , and the  $l$ -resolved DOS,  $N_l(E_F)$  as well as the electron-phonon matrix elements,

$$M_{l,l+1} = -\phi_l(E_F)\phi_{l+1}(E_F) \left[ (D_l(E_F) - l)(D_{l+1}(E_F) + l + 2) + (E_F - V(S))S^2 \right] \quad (4)$$

are calculated from the charge self-consistent potentials obtained with the KKR-ASA CPA method. In Eq. (4),  $\phi_l(E_F)$  is the amplitude of the  $l$ -th partial wave at the sphere boundary,  $S$ , evaluated at  $E_F$ ,  $D_l(E_F)$  is the corresponding logarithmic derivative, and  $V(S)$  is the one-electron potential at  $S$ .

### 3 Results and Discussion

In the following we describe the results of our calculations for  $NbB_2$  and its alloys in terms of (i) the densities of states, (ii) the electron-phonon coupling and (iii) the superconducting transition temperature. We first describe how the densities of states, the electron-phonon coupling and the superconducting transition temperature change for low concentrations of vacancies in either the  $Nb$  or the  $B$  plane. Then, we describe the changes in these properties as a function of increasing vacancy concentration.

#### 3.1 The densities of states of $NbB_2$ , $Nb_{0.99}B_2$ and $NbB_{1.93}$

##### 3.1.1 $NbB_2$

In Fig. 1 we show the calculated total DOS and the partial DOS together with the  $l$ -resolved partial DOS of  $NbB_2$ . The overall structure of the DOS is consistent with the previous work[10,17]. The calculations based on the tight-binding LMTO method yields a value of total DOS at the Fermi energy equal to 4.65 states/Ry-cell [17], while the corresponding value from the full-potential LMTO calculations is found to be 4.28 states/Ry-cell. The present calculations, which is based on the KKR-ASA method, gives  $N(E_F)$  to be equal to 4.41 states/Ry-cell. At  $E_F$  the contributions of  $Nb$  and  $B$  to the total DOS is found to be 3.44 and 0.97 states/Ry-cell, respectively.

The characteristic features in the DOS of  $NbB_2$ , as shown in Fig. 1, are (i) a low lying broad peak around 0.90 – 0.75 Ry below  $E_F$  due to  $B$   $s$ - and  $Nb$   $d$ -states, (ii) another broad peak at around 0.45 – 0.25 Ry comprising of  $B$   $p$ -,  $Nb$   $p$ - and  $Nb$   $d$ - states, (iii) a relatively constant DOS from 0.7 – 0.5 Ry primarily of  $B$   $p$ - and  $Nb$   $d$ - states, and (iv) a pseudo-gap at 0.14 Ry, which appears in many transition-metal diborides [17]. Thus the dominant presence of  $Nb$   $d$ - states at  $E_F$  in  $NbB_2$  makes it quite different from  $MgB_2$  which has largely  $B$   $p$ -states at  $E_F$ .

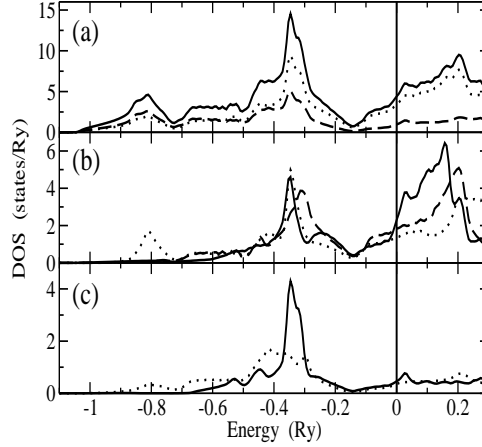


Fig. 1. (a) The total (solid line) and the partial densities of states of  $Nb$  (dotted line) and  $B$  in  $NbB_2$ , calculated with the KKR-ASA CPA method as described in the text. (b) The various symmetry-resolved  $d$ -partial DOS of  $Nb$  in  $NbB_2$  ( $d_{xy}$  : dashed line,  $d_{yz}$  : dotted line and  $d_{3z^2-1}$  : full line). Note that  $d_{x^2-y^2}$  and  $d_{xz}$  are degenerate with  $d_{xy}$  and  $d_{yz}$ , respectively. (c) The symmetry-resolved  $p$ -partial DOS of  $B$  in  $NbB_2$  ( $p_z$  : full line and  $p_x$  : dotted line). In this case,  $p_y$  is degenerate with  $p_x$ .

### 3.1.2 $Nb_{0.99}B_2$

To understand how low concentrations of vacancies in the  $Nb$  plane of  $NbB_2$  would affect its electronic properties, we have used KKR-ASA CPA method to calculate the electronic structure of dilute  $Nb_{1-x}B_2$  with  $x=0.99$  alloy. In this calculation the lattice constants were kept the same as that of  $NbB_2$ . In Fig. 2, we show the calculated  $l$ -resolved partial DOS at the empty sphere site in  $Nb_{0.99}B_2$ . It is seen that upon 1% creation of vacancy in the  $Nb$  plane, the total DOS at  $E_F$  for  $Nb_{0.99}B_2$  is reduced by  $\sim 4\%$  relative to that of  $NbB_2$ . We find that the creation of vacancies in the  $Nb$  plane do not lead to appreciable change in the  $B$  partial DOS at  $E_F$ . Thus the metal deficiency introduced in  $NbB_2$  enhances the ratio of  $B$  states to that of the total DOS at  $E_F$ .

### 3.1.3 $NbB_{1.93}$

Motivated by the work of Otani *et al* on  $NbB_{1.93}$  alloy, which showed that a depletion of  $B$  in  $NbB_2$  led to an increase in the lattice parameter  $c$  from 6.16 to 6.25 a.u. and a decrease in the lattice parameter  $a$  from 5.89 to 5.84 a.u., we have calculated the electronic structure of  $NbB_{1.93}$  alloy. The calculation is carried out by disordering the  $B$  sub-lattice with empty spheres and keeping the  $Nb$  sub-lattice

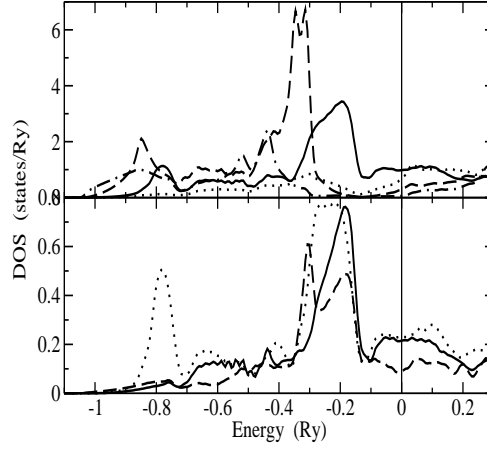


Fig. 2. Top panel: The  $l$ -resolved partial densities of states ( $s$  : dot-dashed line,  $p$  : dashed line,  $d$  : solid line, and  $f$  : dotted line) of the empty sphere in  $Nb_{0.99}B_2$  alloy, calculated with the KKR-ASA CPA method as described in the text. Lower panel: The symmetry-resolved  $d$ -partial DOS of the empty sphere in  $Nb_{0.99}B_2$  ( $d_{xy}$  : full line,  $d_{yz}$  : dotted line and  $d_{3z^2-1}$ : dashed line). Note that  $d_{x^2-y^2}$  and  $d_{xz}$  are degenerate with  $d_{xy}$  and  $d_{yz}$ , respectively.

ordered. The calculated densities of states at  $E_F$  are summarized in Table I, where we have also listed the lattice constants used in the present work.

Our analysis of the DOS of  $NbB_{1.93}$  shows that the creation of vacancies in the  $B$  plane largely reduces the  $d_{3z^2-1}$  component ( $\sim 12.5\%$ ) of the  $Nb$   $d$ -states and the  $B$   $s$ -states ( $\sim 8.9\%$ ) at  $E_F$ . The creation of vacancies in the  $B$  sub lattice of  $NbB_2$  thus leads to a major reduction in those states which are directed along the  $c$ -axis of the unit cell.

Table I. The lattice constants  $a$  and  $c$ , in atomic units, used for  $NbB_2$  and  $NbB_{1.93}$  alloys. The calculated partial ( $Nb$  and  $B$ ) and total densities of states at  $E_F$ , in states/Ry-cell, are also given.

	a	c	$N^{Nb}(E_F)$	$N^B(E_F)$	$N^{tot}(E_F)$
$NbB_2$	5.847	6.259	0.497	3.497	4.491
$NbB_{1.93}$	5.887	6.161	0.473	3.294	4.241

### 3.2 The electron-phonon coupling and the superconducting transition temperature of $NbB_2$ , $Nb_{0.99}B_2$ and $NbB_{1.93}$ alloys

The superconducting transition temperatures of  $NbB_2$ ,  $Nb_{0.99}B_2$  and  $NbB_{1.93}$  were calculated with the Allen-Dynes equation. The factor representing the Coulomb interaction  $\mu^*$  was 0.09. For  $\omega_{rms}$  and  $\omega_{ln}$ , we used the values  $464 \text{ cm}^{-1}$  and  $494 \text{ K}$ , respectively. Our results for the Hopfield parameter  $\eta$ , electron-phonon coupling constant  $\lambda$  and the superconducting transition temperature are summarized in Table II. From Table II, we see that  $\eta_B$ , the Hopfield parameter due to  $B$ , is relatively small in comparison to  $\eta_{Nb}$ , which reflects the fact that  $B$  contribution to the total density of states at  $E_F$  is small. Since we use the same  $\omega_{rms}$  for  $NbB_2$ ,  $Nb_{0.99}B_2$  and  $NbB_{1.93}$  the changes in  $\lambda$  are similar to that of  $\eta$ . The calculated  $T_c$  for  $NbB_2$ ,  $Nb_{0.99}B_2$  and  $NbB_{1.93}$  are found to be 0.31K, 0.13K and 0.004K, respectively. In the case of  $NbB_{1.93}$  alloy, we find that the deficiency of  $B$  largely affects  $\eta_{Nb}$  rather than  $\eta_B$ , which reduces  $T_c$  significantly.

Table II. The calculated Hopfield parameters  $\eta$ , in  $mRy/a_B^2$ , the electron-phonon coupling constant  $\lambda$  and the superconducting transition temperature  $T_c(K)$  for  $NbB_2$  and  $NbB_{1.93}$  alloys. Note that  $\lambda_{tot}=\lambda_{Nb}+2\lambda_B$  for  $NbB_2$  and  $\lambda_{tot}=\lambda_{Nb}+1.93\lambda_B$  for  $NbB_{1.93}$ .

	$\eta_{Nb}$	$\eta_B$	$\lambda_{Nb}$	$\lambda_B$	$\lambda_{tot}$	$T_c$
$NbB_2$	81.7	18.1	0.053	0.121	0.294	0.313
$NbB_{1.93}$	61.2	13.9	0.039	0.089	0.212	0.004

### 3.3 The densities of states of $Nb_{1-x}B_2$ alloys

In Fig. 3, we show the DOS of  $Nb_{0.96}B_2$ ,  $Nb_{0.84}B_2$ ,  $Nb_{0.76}B_2$  and  $Nb_{0.52}B_2$  alloys using the KKR-ASA CPA method. The lattice constants for these alloys were taken from Ref. [4]. The changes in the DOS that arise in  $Nb_{1-x}B_2$  alloys as a function of vacancies are (i) the inward movement of  $E_F$  with increasing vacancy concentration, leading to a decrease in the total DOS at  $E_F$  for  $x < 0.16$  and an increase for  $x > 0.16$ , and (ii) the broadening of peaks with increasing vacancy concentration due to disorder. We find that the movement of  $E_F$  follows the trend as suggested by the rigid-band model, and the DOS of  $Nb_{0.84}B_2$  alloy is similar to  $ZrB_2$ .

### 3.4 The electron-phonon coupling and the superconducting transition temperature of $Nb_{1-x}B_2$ alloys

From the resulting electronic structure we have calculated the variation in the Hopfield parameter, electron-phonon coupling constant and the superconducting transition temperature of  $Nb_{1-x}B_2$  alloys as a function of vacancy concentration. Our

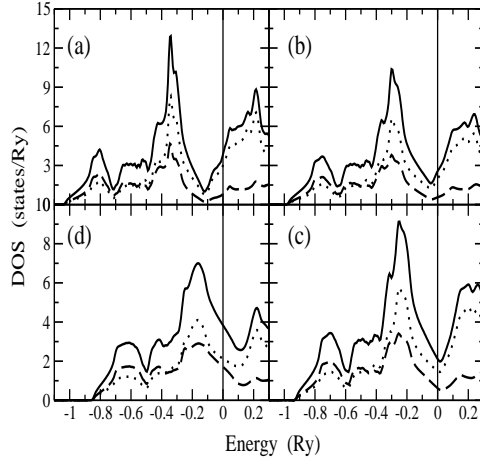


Fig. 3. The total (solid line) and the partial densities of states of  $Nb$  (dotted line) and  $B$  (dashed line) in (a)  $Nb_{0.96}B_2$ , (b)  $Nb_{0.84}B_2$ , (c)  $Nb_{0.76}B_2$  and (d)  $Nb_{0.52}B_2$  alloys, calculated with the KKR-ASA CPA method as described in the text. The vertical line represents the Fermi energy.

results for  $\eta$  and  $\lambda$  are summarized in Table III. We find that both  $\eta$  and  $\lambda$  decrease with increasing vacancy concentration up to  $x \sim 0.25$ , thereafter they start to increase. In Fig. 4, we show the calculated  $T_c$  as a function of  $x$  in  $Nb_{1-x}B_2$  alloys, together with the experimentally reported values. The parameters used in the calculation of  $T_c$  were  $\mu^* = 0.09$ ,  $\omega_{rms} = 400 \text{ cm}^{-1}$ , and  $\omega_{ln} = 494 \text{ K}$ . The calculated trend in the variation of  $T_c$  is in disagreement with the experimental results as shown in Fig. 4. In our opinion, the disagreement is very likely due to the use of a constant  $\omega_{rms}$  value in the Allen-Dynes equation for the whole range of  $x$  from 0 to 0.48 for  $Nb_{1-x}B_2$  alloys.

In the present approach, the calculation of  $T_c$  incorporates two important approximations, (i) use of Gaspari-Gyorffy formalism for estimating the electron-phonon matrix elements, which is known to underestimate the strength of the coupling, and (ii) use of a constant phonon frequency over the whole range of  $x$ . Using Gaspari-Gyorffy formalism with concentration-weighted averages of the phonon frequencies, we have been able to describe reliably the trend in the variation of  $T_c$  in many  $MgB_2$ -based alloys [18,19,20]. Since the electron-phonon coupling in  $NbB_2$  is dominated by  $Nb$  and not by  $B$ , as is the case in  $MgB_2$ , the Gaspari-Gyorffy formalism may be more suitable for  $NbB_2$  than for  $MgB_2$ . This can be seen by comparing the  $T_c$  as calculated in the present approach with that of the linear response calculation of Ref. [11]. The lack of agreement between the present calculations and the observed  $T_c$  in  $Nb_{1-x}B_2$  alloys as a function of  $x$  indicates the importance of incorporating the lattice-dynamical effects in these calculations.



Table III. The calculated variation of Hopfield parameters  $\eta$ , in  $mRy/a_B^2$  and the electron-phonon coupling constant  $\lambda$  as a function of  $x$  in  $Nb_{1-x}B_2$  alloys. Note that  $\lambda_{tot}=(1-x)\lambda_{Nb}+2\lambda_B$  for  $Nb_{1-x}B_2$  alloys.

	$\eta_{Nb}$	$\eta_B$	$\lambda_{Nb}$	$\lambda_B$	$\lambda_{tot}$
$NbB_2$	80.3	21.1	0.070	0.158	0.387
$Nb_{0.96}B_2$	73.1	18.2	0.063	0.136	0.334
$Nb_{0.92}B_2$	65.2	15.4	0.057	0.115	0.283
$Nb_{0.84}B_2$	55.9	12.4	0.048	0.092	0.227
$Nb_{0.76}B_2$	47.6	12.9	0.041	0.097	0.228
$Nb_{0.68}B_2$	62.9	21.0	0.054	0.157	0.356
$Nb_{0.60}B_2$	73.3	27.3	0.064	0.205	0.454
$Nb_{0.52}B_2$	82.2	32.1	0.072	0.241	0.526

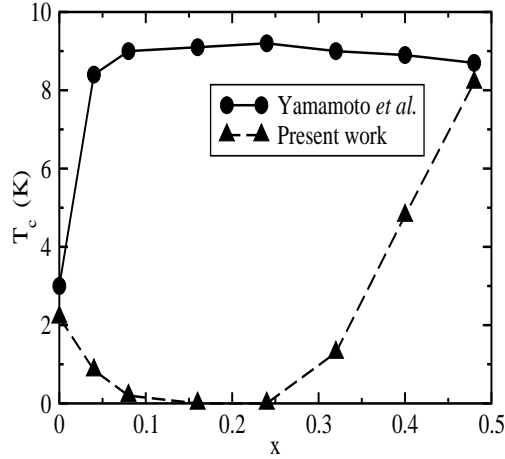


Fig. 4. The calculated (filled triangle) and the observed (filled circle) superconducting transition temperature  $T_c$  of  $Nb_{1-x}B_2$  alloys as a function of  $x$ .

#### 4 Conclusions

We have studied the electronic structure of  $NbB_2$ ,  $NbB_{1.93}$  and  $Nb_{1-x}B_2$  alloys using the KKR-ASA CPA method. We find that the vacancies on the metal plane reduce the number of  $Nb$   $d$ -states at  $E_F$ . The changes in the density of states in  $Nb_{1-x}B_2$  alloys as a function of  $x$  reflect a rigid-band picture. The variation in  $T_c$  in  $Nb_{1-x}B_2$  alloys as a function of  $x$ , calculated using the Gaspari-Gyorffy formalism disagrees with the observed trend. In our opinion, this disagreement arises due to the use of a constant  $\omega_{rms}$  in the Allen-Dynes equation over the whole concentration range in our calculations.

## References

- [1] W. A. Zeigler, R. Young, Phys. Rev. 94 (1953) 115.
- [2] J. K. Hulm, B. T. Mathias, Phys. Rev. 82 (1951) 273.
- [3] J. E. Schriber, D. L. Overmeyer, B. Morosin, E. L. Venturini, R. Baughman, D. Emin, H. Klesnar, T. Aselage, Phys. Rev. B 45 (1992) 10787.
- [4] A. Yamamoto, C. Takao, T. Masui, M. Izumi, S. Tajima, cond-mat/0208331.
- [5] H. Kotegawa, K. Ishida, Y. Kitaoka, T. Muranaka, N. Nakagawa, H. Takagiwa, J. Akimitsu, Physica C 378-381 (2002) 25.
- [6] P. P. Singh, A. Gonis, Phys. Rev. B 49 (1994) 1642.
- [7] J. Faulkner, Prog. Mat. Sci. 27 (1982) 1.
- [8] G. Gaspari, B. L. Gyorffy, Phys. Rev. Lett. 28 (1972) 801.
- [9] P. B. Allen, R. C. Dynes, Phys. Rev. B 12 (1975) 905.
- [10] I. R. Shein, A. L. Ivanovskii, cond-mat/0109445.
- [11] P. P. Singh, Solid State Commun. 125 (2003) 323.
- [12] P. Soven, Phys. Rev. 156 (1967) 809.
- [13] D. Taylor, Phys. Rev. 156 (1967) 1017.
- [14] S. Kirkpatrick, H. E. B. Vellicky, Phys. Rev. B 1 (1970) 3250.
- [15] J. P. Perdew, Y. Wang, Phys. Rev. B 45 (1992) 13244.
- [16] J. P. Perdew, K. Burke, M. Ernzerhof, Phys. Rev. Lett. 77 (1996) 3865.
- [17] P. Vajeeston, P. Ravindran, C. Ravi, R. Asokamani, Phys. Rev. B 63 (2001) 0245115.
- [18] P. J. T. Joseph, P. P. Singh, Solid State Commun. 121 (2002) 467.
- [19] P. P. Singh, Physica C 382 (2002) 381.
- [20] P. P. Singh, P. J. T. Joseph, J. Phys.:Condens. Matter 14 (2001) 12441.